

Cosmological CPT Violation and CMB Polarization Measurements

Jun-Qing Xia

Scuola Internazionale Superiore di Studi Avanzati, Via Bonomea 265, I-34136 Trieste, Italy

(Dated: February 7, 2018)

In this paper we study the possibility of testing Charge-Parity-Time Reversal (CPT) symmetry with cosmic microwave background (CMB) experiments. We consider two kinds of Chern-Simons (CS) term, electromagnetic CS term and gravitational CS term, and study their effects on the CMB polarization power spectra in detail. By combining current CMB polarization measurements, the seven-year WMAP, BOOMERanG 2003 and BICEP observations, we obtain a tight constraint on the rotation angle $\Delta\alpha = -2.28 \pm 1.02$ deg (1σ), indicating a 2.2σ detection of the CPT violation. Here, we particularly take the systematic errors of CMB measurements into account. After adding the QUaD polarization data, the constraint becomes $-1.34 < \Delta\alpha < 0.82$ deg at 95% confidence level. When comparing with the effect of electromagnetic CS term, the gravitational CS term could only generate TB and EB power spectra with much smaller amplitude. Therefore, the induced parameter ϵ can not be constrained from the current polarization data. Furthermore, we study the capabilities of future CMB measurements, Planck and CMBPol, on the constraints of $\Delta\alpha$ and ϵ . We find that the constraint of $\Delta\alpha$ can be significantly improved by a factor of 15. Therefore, if this rotation angle effect can not be taken into account properly, the constraints of cosmological parameters will be biased obviously. For the gravitational CS term, the future Planck data still can not constrain ϵ very well, if the primordial tensor perturbations are small, $r < 0.1$. We need the more accurate CMBPol experiment to give better constraint on ϵ .

PACS numbers: 98.80.Cq, 98.80.Es, 11.30.Cp, 11.30.Er

I. INTRODUCTION

In the standard model of particle physics, Charge-Parity-Time Reversal (CPT) symmetry is a fundamental symmetry. Probing its violation is an important way to search for the new physics beyond the standard model. Up to now, CPT symmetry has passed a number of high-precision experimental tests and no definite signal of its violation has been observed in the laboratory. So, the present CPT violating effects, if they exist, should be very small to be amenable to the experimental limits.

However, the CPT symmetry could be dynamically violated in the expanding universe. In the literature [1–5], the cosmological CPT violation mechanism has an interesting feature, which is that the CPT violating effects at present are too small to be detected by the laboratory experiments, but large enough in the early universe to account for the generation of matter-antimatter asymmetry. More importantly, these types of CPT violating effects could be accumulated to be observable in the cosmological experiments [4–6]. With the accumulation of high-quality observational data, especially those from the cosmic microwave background (CMB) experiments, cosmological observation becomes a powerful way to test the CPT symmetry.

In this paper we firstly consider the cosmological CPT violation in the photon sector where the electrodynamics is modified by a Chern-Simons term $\mathcal{L}_{\text{eCS}} \sim p_\mu A_\nu \bar{F}^{\mu\nu}$. Here, p_μ is an external vector and $\bar{F}^{\mu\nu} = (1/2)\epsilon^{\mu\nu\rho\sigma} F_{\rho\sigma}$ is the dual of the electromagnetic tensor. This term violates the Lorentz and CPT symmetries if p_μ is treated as an external field. One of the physical consequences of this electromagnetic Chern-Simons (eCS) term is the rotation of the polarization direction of electromagnetic waves propagating over large distances [7], which is known as “cosmological birefringence”. This rotation angle $\Delta\alpha$ can be obtained by observing polarized radiation from distant sources such as radio galaxies, quasars, and CMB. For the standard theory of CMB, the TB and EB cross-correlation power spectra vanish. In the presence of the non-zero rotation angle $\Delta\alpha$, one expects to observe non-zero TB and EB power spectra, even if they are zero at the last scattering surface. Denoting the rotated quantities with a prime, one gets [6, 8]

$$\begin{aligned} C_\ell'^{\text{TB}} &= C_\ell^{\text{TE}} \sin(2\Delta\alpha) , \\ C_\ell'^{\text{EB}} &= \frac{1}{2}(C_\ell^{\text{EE}} - C_\ell^{\text{BB}}) \sin(4\Delta\alpha) , \\ C_\ell'^{\text{TE}} &= C_\ell^{\text{TE}} \cos(2\Delta\alpha) , \\ C_\ell'^{\text{EE}} &= C_\ell^{\text{EE}} \cos^2(2\Delta\alpha) + C_\ell^{\text{BB}} \sin^2(2\Delta\alpha) , \\ C_\ell'^{\text{BB}} &= C_\ell^{\text{BB}} \cos^2(2\Delta\alpha) + C_\ell^{\text{EE}} \sin^2(2\Delta\alpha) , \end{aligned} \tag{1}$$

while the CMB temperature power spectrum remains unchanged. Hence we can use the CMB polarization measurements to test the Lorentz and CPT symmetries in this eCS model (see Refs.[4–6, 8–18], and references within). With

homogeneous and isotropic rotation angle, Ref.[15] used the newly released CMB observations and found that a non-zero rotation angle $\Delta\alpha = -2.2 \pm 0.8$ deg (1σ) is favored by the CMB polarization data from the seven-year WMAP (WMAP7) [14], BOOMERanG 2003 (B03) [19] and BICEP [20] observations.

Besides the eCS term, the gravitational Chern-Simons (gCS) term could also generate the non-zero CMB TB and EB cross-correlation power spectra. Following Refs.[21–23], here we consider a Lorentz and CPT violating term in the gravity sector $\mathcal{L}_{\text{gcs}} \sim \epsilon^{\mu\nu\rho\sigma} R_{\beta\mu\nu}^\alpha R_{\alpha\rho\sigma}^\beta$, where $R_{\beta\mu\nu}^\alpha$ is the Riemann tensor. This gCS term does not affect the evolution of background and scalar perturbations. Therefore, the effect of gCS term only appears in the evolution of tensor perturbations, if we neglect the vector perturbations. As we know, the gravitational wave has two independent polarized components denoted by $+$ and \times . We usually use the right- and left-handed circular polarized components:

$$h^{\text{R}} = \frac{1}{\sqrt{2}}(h^+ - ih^\times), \quad h^{\text{L}} = \frac{1}{\sqrt{2}}(h^+ + ih^\times). \quad (2)$$

The power spectra for different handedness are defined as: $\langle h^{s*}(\mathbf{k}_1)h^{s'}(\mathbf{k}_2) \rangle = P_h^{ss'}\delta^3(\mathbf{k}_1 - \mathbf{k}_2)\delta_{ss'}$, where superscripts s and s' stand for the circular polarized state, $s, s' = \text{R}, \text{L}$. Due to the presence of this gCS term, the produced power spectra P_h^{R} and P_h^{L} are not equal. Similarly with Refs.[21–23], we use a parameter ϵ to characterize this discrepancy:

$$\begin{aligned} P_h^{\text{R}} &= \frac{1}{2}P_h(1 - \epsilon) \quad , \quad P_h^{\text{L}} = \frac{1}{2}P_h(1 + \epsilon) \quad , \\ P_h^{\text{R}} + P_h^{\text{L}} &= P_h \quad , \quad P_h^{\text{R}} - P_h^{\text{L}} = -\epsilon P_h \quad . \end{aligned} \quad (3)$$

We can see that $\epsilon = -1, 0, 1$ denote purely right-handed polarized, unpolarized and purely left-handed polarized gravitational wave, respectively. In this paper we only consider the scale-independent ϵ simply.

The CMB power spectra generated by the tensor perturbations are given by:

$$\begin{aligned} C_\ell^{\text{XX}'} &= (4\pi)^2 \int k^2 dk [P_h^{\text{R}}(k) + P_h^{\text{L}}(k)] \Delta_\ell^{\text{X}}(k) \Delta_\ell^{\text{X}'}(k) = (4\pi)^2 \int k^2 dk P_h(k) \Delta_\ell^{\text{X}}(k) \Delta_\ell^{\text{X}'}(k) \quad , \\ C_\ell^{\text{YY}'} &= (4\pi)^2 \int k^2 dk [P_h^{\text{R}}(k) - P_h^{\text{L}}(k)] \Delta_\ell^{\text{Y}}(k) \Delta_\ell^{\text{Y}'}(k) = -(4\pi)^2 \epsilon \int k^2 dk P_h(k) \Delta_\ell^{\text{Y}}(k) \Delta_\ell^{\text{Y}'}(k) \quad , \end{aligned} \quad (4)$$

where XX' and YY' denote TT, TE, EE, BB and TB, EB, respectively, and $\Delta_\ell^{\text{X}}(k)$ are the transfer functions. These equations show that the TT, TE, EE and BB power spectra only depend on the sum of the primordial power spectra of gravitational waves, while the TB and EB power spectra rely on the difference between the power spectra of right- and left-handed polarized components $-\epsilon P_h$. Therefore, in the presence of the gCS term, the non-zero TB and EB correlations will be generated and other four power spectra are unchanged.

In this paper we will study the effects of eCS and gCS terms on the CMB power spectra in detail and perform a global analysis on them by using the latest CMB polarization measurements, as well as the future simulated CMB data. The structure of the paper is as follows: in section II we describe the current and future simulated datasets we use. Section III contains our main results from the current observations and future measurements, while section IV is dedicated to the conclusions and discussion.

II. CMB DATASETS

A. Current Datasets

In our calculations we mainly use the full data of WMAP7 temperature and polarization power spectra [14]. The WMAP7 polarization data are composed of TE/TB/EE/BB/EB power spectra on large scales ($2 \leq \ell \leq 23$) and TE/TB power spectra on small scales ($24 \leq \ell \leq 800$), while the WMAP7 temperature data are only used to set the underlying cosmology. For the systematic error, the WMAP instrument can measure the polarization angle to within ± 1.5 deg of the design orientation [24]. In the computation we use the routines for computing the likelihood supplied by the WMAP team. Besides the WMAP7 information, we also use some small-scale CMB observations.

The *BOOMERanG dated January 2003 Antarctic flight* [19] measures the small-scale CMB polarization power spectra in the range of $150 \leq \ell \leq 1000$. Recently, the BOOMERanG collaboration re-analyzed the CMB power spectra and took into account the effect of systematic errors rotating the polarization angle by -0.9 ± 0.7 deg [25].

Recently, the *Background Imaging of Cosmic Extragalactic Polarization* (BICEP) [20] and *QU Extragalactic Survey Telescope at DASI* (QUaD) [26] collaborations released their high precision data of the CMB temperature and polarization including the TB and EB power spectra. These two experiments, locating at the South Pole, are the bolometric polarimeters designed to capture the CMB information at two different frequency bands of 100GHz and

TABLE I: Assumed experimental specifications. We use the CMB power spectra only at $l \leq 2500$. The noise parameters Δ_T and Δ_P are given in units of $\mu\text{K-arcmin}$.

Experiment	f_{sky}	ℓ_{max}	(GHz)	θ_{FWHM}	Δ_T	Δ_P
PLANCK	0.65	2500	100	9.5'	6.8	10.9
			143	7.1'	6.0	11.4
			217	5.0'	13.1	26.7
CMBPol	0.65	2500	217	3.0'	1.0	1.4

150GHz, and on small scales – the released first two-year BICEP data are in the range of $21 \leq \ell \leq 335$ [20]; whereas the QUaD team measures the polarization spectra at $164 \leq \ell \leq 2026$, based on an analysis of the observation in the second and third season [12, 13]. They also provide the systematic errors of measuring the polarization angle, ± 0.7 deg and ± 0.5 deg, for BICEP and QUaD observations, respectively.

B. Future Datasets

Current CMB measurements are still not accurate enough to verify the possible CPT violation. We follow the method given in Refs.[9, 17] and simulate the CMB power spectra with the assumed experimental specifications of the future Planck [27] and CMBPol [28] measurements. We choose the best-fit model from the WMAP7 data [14] as the fiducial model.

In Table I we list the assumed experimental specifications of the future Planck and CMBPol measurements. The likelihood function is $\mathcal{L} \propto \exp(-\chi_{\text{eff}}^2/2)$ and

$$\chi_{\text{eff}}^2 = \sum_{\ell} (2\ell + 1) f_{\text{sky}} \left(\frac{A}{|\bar{C}|} + \ln \frac{|\bar{C}|}{|\hat{C}|} + 3 \right), \quad (5)$$

where f_{sky} denotes the observed fraction of the sky in the real experiments, A is defined as:

$$\begin{aligned} A = & \hat{C}_{\ell}^{TT} (\bar{C}_{\ell}^{EE} \bar{C}_{\ell}^{BB} - (\bar{C}_{\ell}^{EB})^2) + \hat{C}_{\ell}^{TE} (\bar{C}_{\ell}^{TB} \bar{C}_{\ell}^{EB} - \bar{C}_{\ell}^{TE} \bar{C}_{\ell}^{BB}) \\ & + \hat{C}_{\ell}^{TB} (\bar{C}_{\ell}^{TE} \bar{C}_{\ell}^{EB} - \bar{C}_{\ell}^{TB} \bar{C}_{\ell}^{EE}) + \hat{C}_{\ell}^{TE} (\bar{C}_{\ell}^{TB} \bar{C}_{\ell}^{EB} - \bar{C}_{\ell}^{TE} \bar{C}_{\ell}^{BB}) \\ & + \hat{C}_{\ell}^{EE} (\bar{C}_{\ell}^{TT} \bar{C}_{\ell}^{BB} - (\bar{C}_{\ell}^{TB})^2) + \hat{C}_{\ell}^{EB} (\bar{C}_{\ell}^{TE} \bar{C}_{\ell}^{TB} - \bar{C}_{\ell}^{TT} \bar{C}_{\ell}^{EB}) \\ & + \hat{C}_{\ell}^{TB} (\bar{C}_{\ell}^{TE} \bar{C}_{\ell}^{EB} - \bar{C}_{\ell}^{EE} \bar{C}_{\ell}^{TB}) + \hat{C}_{\ell}^{EB} (\bar{C}_{\ell}^{TE} \bar{C}_{\ell}^{TB} - \bar{C}_{\ell}^{TT} \bar{C}_{\ell}^{EB}) \\ & + \hat{C}_{\ell}^{BB} (\bar{C}_{\ell}^{TT} \bar{C}_{\ell}^{EE} - (\bar{C}_{\ell}^{TE})^2), \end{aligned} \quad (6)$$

and $|\bar{C}|$ and $|\hat{C}|$ denote the determinants of the theoretical and observed data covariance matrices respectively,

$$\begin{aligned} |\bar{C}| = & \bar{C}_{\ell}^{TT} \bar{C}_{\ell}^{EE} \bar{C}_{\ell}^{BB} + 2\bar{C}_{\ell}^{TE} \bar{C}_{\ell}^{TB} \bar{C}_{\ell}^{EB} - \bar{C}_{\ell}^{TT} (\bar{C}_{\ell}^{EB})^2 \\ & - \bar{C}_{\ell}^{EE} (\bar{C}_{\ell}^{TB})^2 - \bar{C}_{\ell}^{BB} (\bar{C}_{\ell}^{TE})^2, \\ |\hat{C}| = & \hat{C}_{\ell}^{TT} \hat{C}_{\ell}^{EE} \hat{C}_{\ell}^{BB} + 2\hat{C}_{\ell}^{TE} \hat{C}_{\ell}^{TB} \hat{C}_{\ell}^{EB} - \hat{C}_{\ell}^{TT} (\hat{C}_{\ell}^{EB})^2 \\ & - \hat{C}_{\ell}^{EE} (\hat{C}_{\ell}^{TB})^2 - \hat{C}_{\ell}^{BB} (\hat{C}_{\ell}^{TE})^2. \end{aligned} \quad (7)$$

The likelihood has been normalized with respect to the maximum likelihood $\chi_{\text{eff}}^2 = 0$, where $\bar{C}_{\ell}^{\text{XY}} = \hat{C}_{\ell}^{\text{XY}}$.

III. NUMERICAL RESULTS

In our study we make a global analysis to the CMB data with the public available Markov Chain Monte Carlo package `CosmoMC` [29], which has been modified to compute the non-zero TB and EB power spectra discussed above. We assume the purely adiabatic initial conditions and impose the flatness condition motivated by inflation. Our basic parameter space is: $\mathbf{P} \equiv (\omega_b, \omega_c, \Omega_{\Lambda}, \tau, n_s, A_s, r)$, where $\omega_b \equiv \Omega_b h^2$ and $\omega_c \equiv \Omega_c h^2$ are the physical baryon and cold dark matter densities relative to the critical density, Ω_{Λ} is the dark energy density relative to the critical density, τ

TABLE II: Constraints on the rotation angle $\Delta\alpha$ (68% C.L.) from various CMB data combinations.

CMB Data sets	without systematics	with systematics
WMAP7	-1.06 ± 1.39 deg	-1.14 ± 2.05 deg
B03	-5.97 ± 4.05 deg	-4.63 ± 4.16 deg
BICEP	-2.59 ± 0.99 deg	-2.57 ± 1.21 deg
QUaD	0.60 ± 0.40 deg	0.59 ± 0.64 deg
WMAP7+B03+BICEP	-2.23 ± 0.83 deg	-2.28 ± 1.02 deg
WMAP7+BICEP+QUaD	0.07 ± 0.36 deg	-0.22 ± 0.54 deg
WMAP7+B03+BICEP+QUaD	0.04 ± 0.34 deg	-0.26 ± 0.54 deg

is the optical depth to re-ionization, A_s and n_s characterize the primordial scalar power spectrum, r is the tensor to scalar ratio of the primordial spectrum. For the pivot of the primordial spectrum we set $k_{s0} = 0.002 \text{ Mpc}^{-1}$. Furthermore, in our analysis we include the CMB lensing effect, which also produces B modes from E modes [30], when we calculate the theoretical CMB power spectra.

A. Electromagnetic Chern-Simons Term

Firstly, we consider the constraint on the rotation angle $\Delta\alpha$, induced by the eCS term, from the current CMB measurements. As we know, this rotation angle is accumulated along the journey of CMB photons, and the constraints on the rotation angle depends on the multipoles ℓ [16]. Refs.[10, 14] found that the rotation angle is mainly constrained from the high- ℓ polarization data, and the polarization data at low multipoles do not affect the result significantly. Therefore, in our analysis, we assume a constant rotation angle $\Delta\alpha$ at all multipoles. Further, we also impose a conservative flat prior on $\Delta\alpha$ as, $-\pi/2 \leq \Delta\alpha \leq \pi/2$.

In our previous works, we only presented the statistical errors of rotation angle and did not consider the possible systematic errors of CMB measurements. Inspired by Ref.[25], in this paper we consider two rotation angles, $\Delta\alpha$ and β , in order to take into account the real rotation signal and a systematic error for each CMB polarization measurement. Therefore, in our analyses we have five free parameters in this eCS model: the rotation angle signal $\Delta\alpha$ and four systematic errors, $\beta_{\text{WMAP7}}, \beta_{\text{B03}}, \beta_{\text{BICEP}}, \beta_{\text{QUaD}}$, for four CMB observations, respectively. And we impose priors on these four systematic errors:

$$\begin{aligned} \beta_{\text{WMAP7}} &= 0.0 \pm 1.5 \text{ deg} , & \beta_{\text{B03}} &= -0.9 \pm 0.7 \text{ deg} , \\ \beta_{\text{BICEP}} &= 0.0 \pm 0.7 \text{ deg} , & \beta_{\text{QUaD}} &= 0.0 \pm 0.5 \text{ deg} , \end{aligned} \quad (8)$$

and marginalize over them to constrain the rotation angle. In Table II we present current constraints on $\Delta\alpha$ from the WMAP7, B03, BICEP and QUaD CMB polarization power spectra with and without CMB systematic errors.

When only using WMAP7 power spectra data at all multipoles ℓ , without the systematic effect ($\beta_{\text{WMAP7}} = 0$), we obtain the constraint on the rotation angle: $\Delta\alpha = -1.06 \pm 1.39$ deg at 68% confidence level, which is quite consistent with that obtained from the WMAP team [14] and is a significant improvement over the WMAP3 [9] and WMAP5 [10, 11] results. After adding the prior of β_{WMAP7} into the χ^2 calculation, the constraint becomes weaker: $\Delta\alpha = -1.14 \pm 2.05$ deg (68% C.L.) and $-5.24 < \Delta\alpha < 2.96$ deg (95% C.L.). Similarly, we revisit the constraint on $\Delta\alpha$ from the B03 polarization data and obtain the constraints at 68% C.L.: $\Delta\alpha = -5.97 \pm 4.05$ deg and $\Delta\alpha = -4.63 \pm 4.16$ deg, without and with the CMB systematic effect, respectively. The results are in good agreement with the previous results of Refs.[6, 25]. These two CMB measurements show a weak indication for a non-zero rotation angle about 1σ confidence level.

Recently, BICEP and QUaD collaborations also released their high precision CMB polarization data. In our previous work [15], we found that the BICEP data alone could give very tight constraint on the rotation angle: $\Delta\alpha = -2.59 \pm 0.99$ deg (68% C.L.), when fixing $\beta_{\text{BICEP}} = 0$, which means that BICEP data alone favors a non-zero rotation angle at about 2.5σ confidence level. When we include the systematic effect of BICEP measurement, the constraints at 68% and 95% C.L. are:

$$\Delta\alpha = -2.57 \pm 1.21 \text{ deg (68% C.L.)} , \quad -4.99 < \Delta\alpha < -0.15 \text{ deg (95% C.L.)} , \quad (9)$$

which still gives a more than 2σ detection of a non-vanishing rotation angle. Furthermore, when WMAP7 and B03 data are added to the BICEP sample, the constraint on $\Delta\alpha$ gets tightened:

$$\Delta\alpha = -2.28 \pm 1.02 \text{ deg (68% C.L.)} , \quad -4.32 < \Delta\alpha < -0.24 \text{ deg (95% C.L.)} , \quad (10)$$

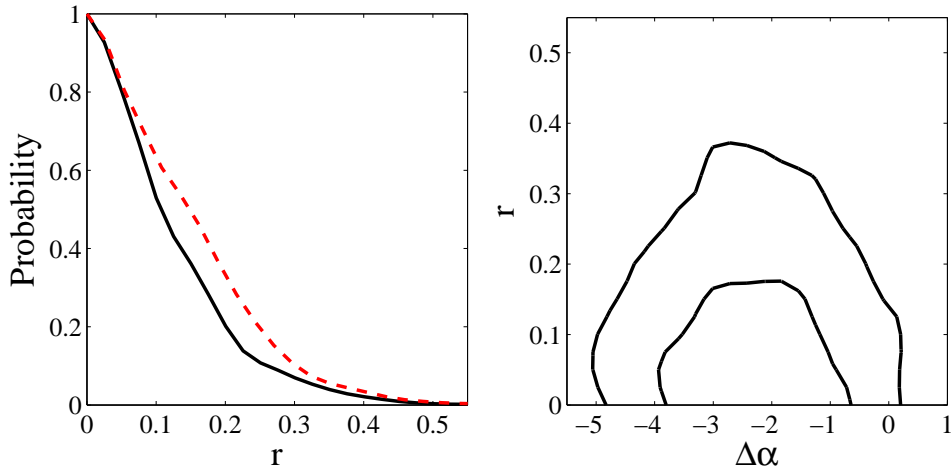


FIG. 1: Left panel: The one-dimensional posterior distributions of the tensor to scalar ratio r derived from the WMAP7+B03+BICEP data combinations including (black solid line) and not including (red dashed line) the rotation angle. Right panel: Two-dimensional $1, 2\sigma$ contours in the $\Delta\alpha - r$ plane.

which implies $\Delta\alpha \neq 0$ at 2.2σ confidence level, even considering systematic effects of these three CMB measurements.

Finally, we constrain the rotation angle from the QUaD polarization data. Similarly with previous results of QUaD collaboration, we use the QUaD data alone and obtain the constraint at 68% confidence level without and with systematic effect: $\Delta\alpha = 0.60 \pm 0.40$ deg and $\Delta\alpha = 0.59 \pm 0.64$ deg, respectively. When comparing with the result of WMAP7+B03+BICEP [Eq.(10)], there is a $\sim 2\sigma$ tension between QUaD and WMAP7+B03+BICEP observations, no matter whether we include the systematic effects of these CMB measurements. As we discussed before [15], this tension should be taken care of in the further investigation. By combining WMAP7, BICEP and QUaD data and including their systematic effects, we obtain the constraint: $\Delta\alpha = -0.22 \pm 0.54$ deg (68% C.L.) and $-1.30 < \Delta\alpha < 0.86$ deg (95% C.L.), which is consistent with the result of Ref.[14]. When adding the B03 data into the analysis, the constraint on the rotation angle does not change significantly, due to large error bars of B03 polarization data.

Moreover, the sources of the CMB polarization, especially for the B-mode, are not unique. For example, the B-mode can be generated by the cosmological birefringence as mentioned above; it might be converted from E-mode by cosmic shear [30]; it could be the signature of the gravitational waves; or it can even be produced by the instrumental systematics. Therefore, one should bear in mind that the rotation angle might be degenerate with other cosmological parameters or nuisance parameters when fitted to the polarization data. Therefore, in order to distinguish these effects and obtain the clean information of the primordial tensor B-mode, the rotation angle has to be constrained, and the measurements of TB and EB power spectra are really necessary. Otherwise, the constraints of cosmological parameters might be biased, if this cosmological birefringence effect can not be taken into account properly. In the left panel of Fig.1 we show the one-dimensional posterior distributions of the tensor to scalar ratio r derived from the WMAP7+B03+BICEP data combinations. When including the rotation angle, the 95% upper limit of r is: $r < 0.26$, while we obtain $r < 0.29$ with $\Delta\alpha = 0$. Since the data combination WMAP7+B03+BICEP favors a negative rotation angle which contributes the BB power spectrum, the BB power spectrum from primordial tensor perturbations, as well as the upper limit of r , will be slightly suppressed, consequently. We also show the two-dimensional contour between the tensor and the rotation angle in the right panel of Fig.1. Due to the large error bars of current CMB polarization data, the effect of non-zero rotation angle is neglectable on the constraints of cosmological parameters. However, this effect might be important in the future forecasts.

Therefore, we simulate the future CMB power spectra with Planck to investigate the effect of non-zero rotation angle on the constraints of cosmological parameters. The fiducial model we choose is the best-fit WMAP7 model [14]: $\Omega_b h^2 = 0.023$, $\Omega_c h^2 = 0.108$, $\Omega_\Lambda = 0.752$, $\tau = 0.087$, $n_s = 0.98$, and $\log[10^{10} A_s] = 3.135$ at $k_{s0} = 0.002 \text{ Mpc}^{-1}$. For the tensor to scalar ratio r , we have two fiducial models: $r = 0$ and $r = 0.3$. For each model, we consider three fiducial values of the rotation angle with $\Delta\alpha = 0, -2, -5$ deg. Here, we neglect the systematic error of future CMB measurement and the CMB lensing effect. In Table III we list the constraints on the cosmological parameters with different fiducial models.

When we include the rotation angle in the calculations, as you can see in Table III, the fiducial values of input parameters are always recovered. The future Planck measurement could shrink the standard deviation of rotation

TABLE III: Constraints on the cosmological parameters (68% C.L.) from future CMB mock data.

Parameters	$100\Omega_b h^2$	$10\Omega_c h^2$	$10\Omega_\Lambda$	10τ	$10n_s$	$\log[10^{10}A_s]$	r (95% C.L.)	$\Delta\alpha$ (deg)	$\Delta\chi^2$
Fiducial	2.300	1.080	7.520	0.870	9.800	3.135	See below	See below	0
PLANCK, $r = 0$, $\Delta\alpha$ free									
$\Delta\alpha = 0^\circ$	2.300 ± 0.017	1.079 ± 0.015	7.519 ± 0.077	0.868 ± 0.057	9.804 ± 0.045	3.133 ± 0.019	< 0.033	-0.001 ± 0.058	0
$\Delta\alpha = -2^\circ$	2.301 ± 0.017	1.079 ± 0.015	7.521 ± 0.076	0.870 ± 0.056	9.805 ± 0.043	3.133 ± 0.019	< 0.035	-2.001 ± 0.061	0
$\Delta\alpha = -5^\circ$	2.301 ± 0.017	1.079 ± 0.015	7.520 ± 0.078	0.867 ± 0.057	9.805 ± 0.045	3.133 ± 0.019	< 0.037	-5.000 ± 0.062	0
PLANCK, $r = 0$, $\Delta\alpha \equiv 0$									
$\Delta\alpha = 0^\circ$	2.300 ± 0.017	1.079 ± 0.015	7.518 ± 0.078	0.870 ± 0.057	9.806 ± 0.044	3.133 ± 0.019	< 0.032	—	0
$\Delta\alpha = -2^\circ$	2.304 ± 0.017	1.082 ± 0.015	7.506 ± 0.080	0.868 ± 0.056	9.804 ± 0.045	3.134 ± 0.019	< 0.048	—	6.98
$\Delta\alpha = -5^\circ$	2.327 ± 0.017	1.085 ± 0.015	7.499 ± 0.077	0.858 ± 0.056	9.836 ± 0.044	3.119 ± 0.019	0.081 ± 0.058	—	261.68
PLANCK, $r = 0.3$, $\Delta\alpha$ free									
$\Delta\alpha = 0^\circ$	2.300 ± 0.017	1.080 ± 0.015	7.512 ± 0.078	0.870 ± 0.056	9.801 ± 0.045	3.135 ± 0.020	0.305 ± 0.100	0.003 ± 0.060	0
$\Delta\alpha = -2^\circ$	2.300 ± 0.016	1.080 ± 0.015	7.513 ± 0.077	0.871 ± 0.056	9.802 ± 0.044	3.135 ± 0.020	0.308 ± 0.100	-2.003 ± 0.059	0
$\Delta\alpha = -5^\circ$	2.300 ± 0.017	1.080 ± 0.015	7.513 ± 0.076	0.873 ± 0.057	9.800 ± 0.044	3.136 ± 0.020	0.303 ± 0.102	-4.998 ± 0.059	0
PLANCK, $r = 0.3$, $\Delta\alpha \equiv 0$									
$\Delta\alpha = 0^\circ$	2.300 ± 0.017	1.080 ± 0.015	7.515 ± 0.078	0.872 ± 0.057	9.800 ± 0.045	3.135 ± 0.020	0.309 ± 0.099	—	0
$\Delta\alpha = -2^\circ$	2.303 ± 0.017	1.082 ± 0.015	7.503 ± 0.077	0.863 ± 0.056	9.802 ± 0.045	3.134 ± 0.020	0.317 ± 0.104	—	6.54
$\Delta\alpha = -5^\circ$	2.333 ± 0.017	1.087 ± 0.015	7.491 ± 0.075	0.857 ± 0.056	9.831 ± 0.045	3.121 ± 0.019	0.389 ± 0.104	—	260.74

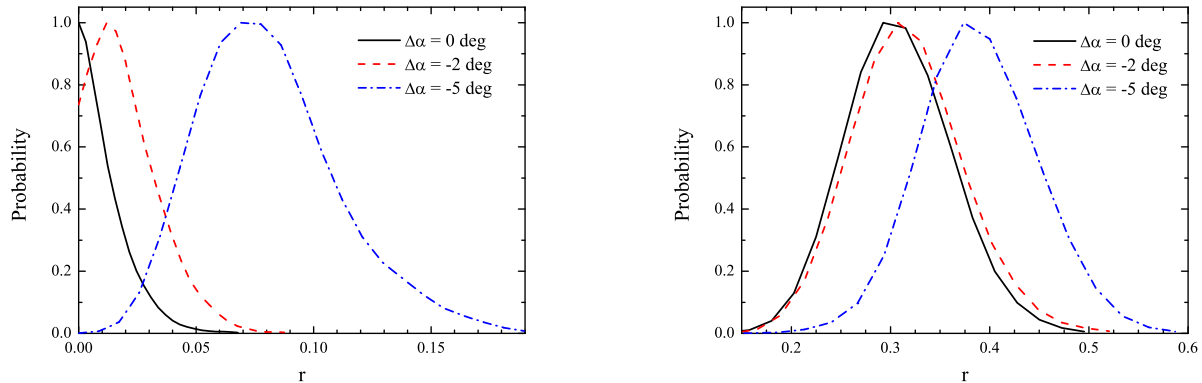


FIG. 2: The one-dimensional posterior distributions of the tensor to scalar ratio r derived from the future Planck mock data without including the rotation angle. The fiducial values of r are 0 (left panel) and 0.3 (right panel). The rotation angles considered in the fiducial model are: $\Delta\alpha = 0$ deg (black solid lines), $\Delta\alpha = -2$ deg (red dashed lines), and $\Delta\alpha = -5$ deg (blue dash-dotted lines).

angle by a factor of 15, namely $\sigma(\Delta\alpha) \simeq 0.06$ deg, which is consistent with our previous results [9, 17]. The non-zero rotation angle and the possible cosmological CPT violation can be verified by the future CMB measurements.

However, if we neglect the effect of rotation angle at all ($\Delta\alpha \equiv 0$), the contribution of non-zero rotation angle on the BB power spectrum will be wrongly considered as the primordial tensor perturbations. For the fiducial model $r = 0$, the BB power spectrum due to the primordial tensor B-mode should vanish. But in the presence of non-zero fiducial rotation angle ($\Delta\alpha = -2, -5$ deg), the BB power spectrum should be non-vanishing. If we force the rotation angle to be zero in the analysis, the value of r will be enlarged to match the mock non-zero BB power spectrum. Using the $\Delta\alpha$ -free cases as the reference model, in Table III we can see that the minimal χ^2 of the cases with $\Delta\alpha \equiv 0$ are extremely larger, which implies that this kind of model does not fit the mock data well. In the left panel of Fig.2, we find that the larger the fiducial value of $\Delta\alpha$ is, the larger the obtained central value of r becomes. Consequently, this large value of r will enhance the CMB TT power spectrum at large scales. The contribution of primordial scalar perturbations on the TT power spectrum will be suppressed, which will change constraints of other cosmological parameters, for example, the baryon energy density $\Omega_b h^2$ becomes larger and the amplitude of primordial scalar perturbations A_s becomes smaller. See the Table III for details. Therefore, if we do not take the effect of rotation angle into account

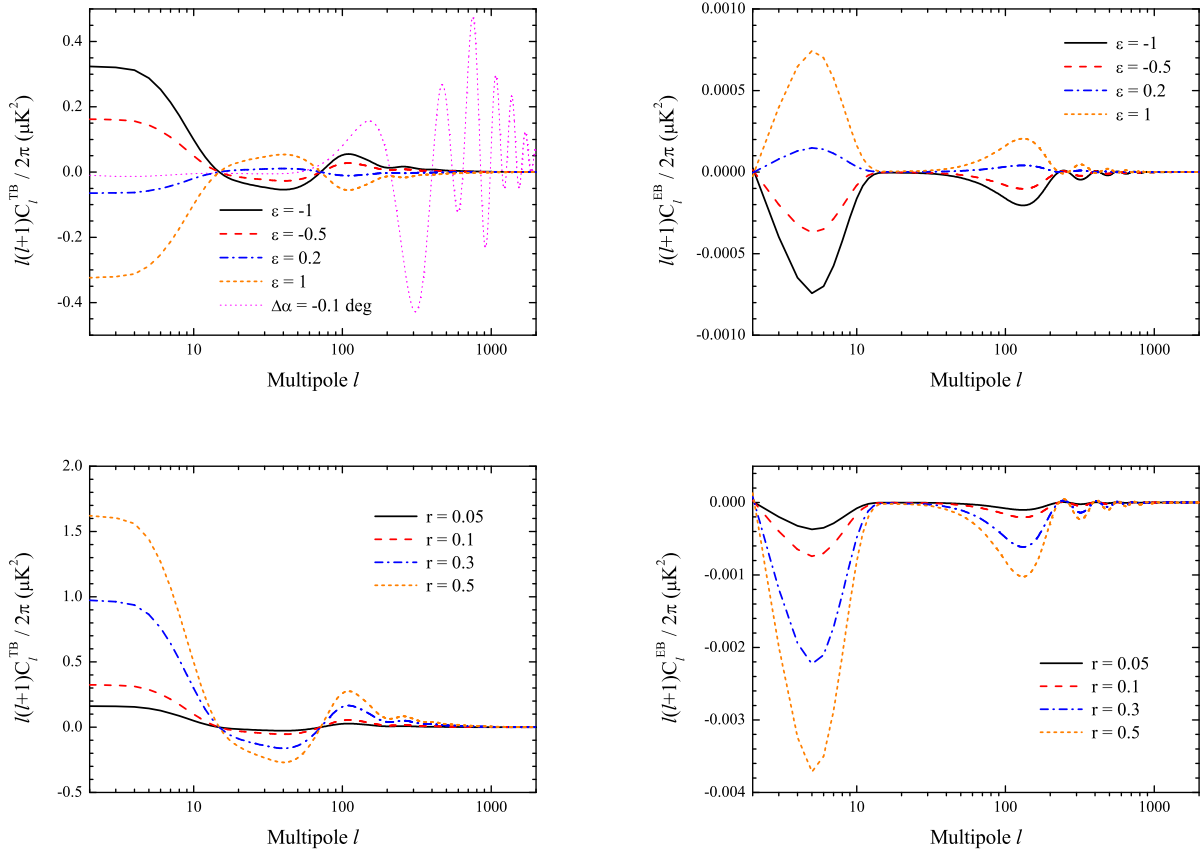


FIG. 3: Upper panels: The theoretical TB and EB power spectra for different values of ϵ with $r = 0.1$. Below panels: The theoretical TB and EB power spectra for different values of r with $\epsilon = -1$. We also show the theoretical TB power spectrum with the rotation angle $\Delta\alpha = -0.1$ deg for comparison in the upper left panel (magenta dotted line).

properly, the constraints of cosmological parameters derived from the future CMB data with high accuracy will be biased. We also find the similar situation for the case with $r = 0.3$ (right panel of Fig.2).

B. Gravitational Chern-Simons Term

In this subsection, we study the effect of gCS term on the CMB power spectra and constrain the parameter ϵ from the CMB polarization data. Note that, in our analyses we do not follow Ref.[22] which took the effects of eCS and gCS terms into account simultaneously, since the current constraint on ϵ is still too weak to consider this kind of degeneracy. We always assume the rotation angle $\Delta\alpha = 0$ and neglect the systematic effects of CMB polarization data in the calculations. Therefore, we only have one more free parameter $\epsilon \in [-1, 1]$, induced by the gCS term, and assume that it is scale-independent.

Firstly, we show the effect of the gCS term on the CMB polarization power spectra. As we discuss before, a non-zero ϵ only generates the non-zero TB and EB power spectra and leaves other four power spectra unchanged. In the upper panels of Fig.3, we plot the CMB TB and EB power spectra for different fiducial values of ϵ with $r = 0.1$. We find that the non-zero ϵ mainly affect the TB power spectrum on large scales ($\ell < 200$). There is a significantly enhancement on the amplitude of TB power spectrum on the largest scales ($\ell < 10$), which is related to the CMB reionization information [21]. We also notice that there are only two crossing points around $\ell \sim 15$ and 70 on the TB power spectrum. For comparison, we show the TB power spectrum generated by a rotation angle $\Delta\alpha = -0.1$ deg in the plot (magenta dotted line). As we know, the non-zero rotation angle will generate the TB power spectrum, based on the relation: $C_\ell^{\prime\text{TB}} = C_\ell^{\text{TE}} \sin(2\Delta\alpha)$ which implies that the shape of TB power spectrum is exactly the same with that of TE power spectrum. Therefore, the TB power spectrum with a non-zero $\Delta\alpha$ has many crossing points at high

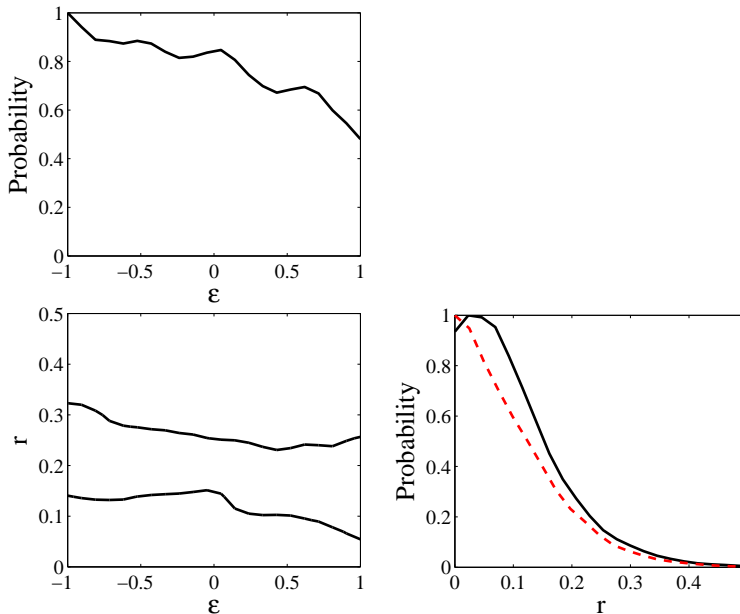


FIG. 4: Marginalized one-dimensional and two-dimensional distributions ($1, 2\sigma$ contours) of ϵ and r . In the right below panel we also show the constraint of r without considering the non-zero gCS term, $\epsilon = 0$ (red dashed line).

multipoles ($\ell > 200$) and its signal mainly comes from the small scales. We could distinguish the TB power spectrum from the eCS term and that from the gCS term clearly on small scales. Moreover, in the plot we only show the TB power spectrum with $\Delta\alpha = -0.1$ deg which is much smaller than the best fit value from WMAP7+B03+BICEP data, $\Delta\alpha \sim -2$ deg, because the signal of TB power spectrum from the eCS term is much higher than that from gCS term, especially on small scales. Thus, if we find very large signal on small scales of TB power spectrum from the future observation, it only could be the signature of a non-zero rotation angle.

We find the similar situation on the EB power spectrum. From the upper right panel of Fig.3, we can see that the effect of the EB power spectrum, induced by the gCS term, is mainly on large scales and becomes to zero at high multipoles. There are many crossing points on the EB power spectrum, while the EB power spectrum, induced by the eCS term, does not have the crossing point. Based on the relation: $C_\ell^{\prime EB} \sim (C_\ell^{EE} - C_\ell^{BB}) \sin(4\Delta\alpha)$, the EB power spectrum can not cross the zero line, since the EE power spectrum is always positive and larger than the BB power spectrum. Here, we do not show the curve in the plot for comparison, since the amplitude of EB power spectrum produced by the eCS term is much larger than that by the gCS term. Thus, the EB power spectrum can also be used to distinguish the eCS and gCS models, if the future CMB polarization data are accurate enough.

In the below two panels of Fig.3, we show the dependence of r on the TB and EB power spectra with $\epsilon = -1$. One can see that the amplitudes of TB/EB power spectra are highly related to by the fiducial value of r , and their shapes remain unchanged. Therefore, the significance of detection of non-zero ϵ will be directly determined by the primordial tensor perturbations r . At present, CMB observations do not detect the signature of non-zero r , which means that results on r are consistent with zero. Consequently, we can not constrain the parameter ϵ very well from the current CMB polarization data, due to the very small primordial tensor perturbations. In Fig.4, we show the constraints on ϵ and r from the WMAP7+B03+BICEP+QUaD data combination after marginalized over other cosmological parameters. From the one-dimensional distribution of ϵ , as well as the flat two-dimensional contours, apparently the present CMB data can not give good constraints on ϵ . There is a peak around $\epsilon = -1$, which implies that a right-hand polarized gravitational wave might be slightly favored. We also show the one-dimensional distribution of r including and not including the free parameter ϵ . Due to the degeneracy between ϵ and r , the constraint on r is slightly relaxed when a free ϵ is included in the calculation.

Thus, we use the same fiducial model in the last subsection to simulate the future Planck polarization data to constrain ϵ . For the tensor to scalar ratio r , we have two fiducial models: $r = 0.1$ and $r = 0.3$. For each model, we consider six fiducial values of ϵ with $\epsilon = 0, -0.2, -0.4, -0.6, -0.8, -1$. In Table IV and upper panels of Fig.5 we show the constraints on ϵ from the future CMB mock data with different fiducial models. If we choose the fiducial value $r = 0.1$, even the Planck mock data can not give good constraint on ϵ (the upper left panel). The 95% confidence

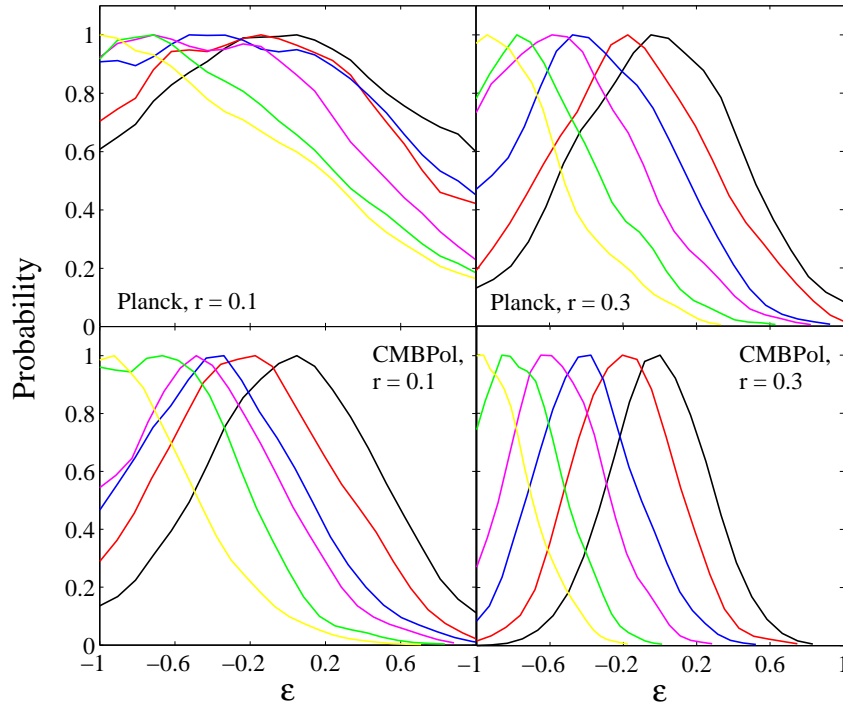


FIG. 5: The one-dimensional posterior distributions of ϵ derived from the future Planck (upper panels) and CMBPol (below panels) measurements with different fiducial models of r . For each case, we have six fiducial values of ϵ : $\epsilon = 0$ (black), -0.2 (red), -0.4 (blue), -0.6 (magenta), -0.8 (green), and -1 (yellow).

TABLE IV: Constraints on ϵ (95% C.L.) from future CMB mock data.

Fiducial ϵ	Planck, $r = 0.1$	Planck, $r = 0.3$	CMBPol, $r = 0.1$	CMBPol, $r = 0.3$
$\epsilon = 0$	$[-1, 1]$	$[-0.69, 0.66]$	$[-0.71, 0.70]$	$[-0.43, 0.42]$
$\epsilon = -0.2$	$[-1, 1]$	$[-1, 0.57]$	$[-1, 0.54]$	$[-0.61, 0.23]$
$\epsilon = -0.4$	$[-1, 1]$	$[-1, 0.32]$	$[-1, 0.37]$	$[-0.80, 0.05]$
$\epsilon = -0.6$	$[-1, 1]$	$[-1, 0.22]$	$[-1, 0.25]$	$[-1, -0.12]$
$\epsilon = -0.8$	$[-1, 1]$	$[-1, 0.02]$	$[-1, 0.03]$	$[-1, -0.36]$
$\epsilon = -1.0$	$[-1, 1]$	$[-1, -0.12]$	$[-1, -0.08]$	$[-1, -0.48]$

levels of ϵ are always $[-1, 1]$ for six fiducial values of ϵ . As we discuss before, the larger the value of r is, the higher the amplitudes of CMB TB/EB power spectra are (the below panels of Fig.3). When the fiducial value of r becomes larger ($r = 0.3$), the constraints on ϵ become better. The standard deviations of ϵ have been shrunk significantly. But the constraints are still not conclusive. Obviously, the future Planck measurement will be very difficult to constrain ϵ , if the primordial tensor perturbations are small, $r < 0.1$. Therefore, we also simulate the future CMBPol polarization data with higher accuracy and re-do the calculations, see Table III and below panels of Fig.5. In this case, even with $r = 0.1$ the CMBPol data could also give good constraints on ϵ . Finally, we obtain the standard deviation of ϵ : $\sigma(\epsilon) \sim 0.1$ with the fiducial value $r = 0.3$. The future CMBPol experiment could constrain ϵ better.

IV. CONCLUSIONS AND DISCUSSIONS

Probing the violation of fundamental symmetries is an important way to search for the new physics beyond the standard model. In this paper we present constraints on the eCS and gCS models using the latest CMB polarization data, as well as the future simulated mock data.

In the constraints of rotation angle, induced by the eCS model, we extend our previous works by including the systematic errors of CMB polarization measurements. We consider two rotation angles, $\Delta\alpha$ and β , in order to take into account the real rotation signal and a systematic error for each CMB polarization measurement, and impose priors on the systematic errors. Adding the systematic effects of CMB polarization data, we do not find significant change on the constraints of $\Delta\alpha$, except the error bars become slightly larger. WMAP7+B03+BICEP data combination still favors a non-zero rotation angle about 2.2σ confidence level, namely $\Delta\alpha = -2.28 \pm 1.02$ (deg), no matter whether the systematic effects are included. We still find a $\sim 2\sigma$ tension between QUaD and WMAP7+B03+BICEP observations. When combining all CMB polarization data together, we obtain the tight constraint on the rotation angle at 95% confidence level: $-1.34 < \Delta\alpha < 0.82$ (deg), which is consistent with a CPT-conserving Universe.

Since the current constraints on the rotation angle are not conclusive, we simulate the future Planck polarization data. We find that the future CMB data could significantly improve the constraint of $\Delta\alpha$ by a factor of 15 ($\sigma(\Delta\alpha) \simeq 0.06$ deg). Because a non-zero rotation angle will generate the BB power spectrum, we need to take this effect into account properly in the future data analysis. Otherwise the constraints of cosmological parameters will be apparently biased.

We also give the constraint on the parameter ϵ , which is induced by the gCS term and denotes the difference between the right- and left-handed polarized components. Since the effects of non-zero ϵ on the TB and EB power spectra are very small, the parameter ϵ is almost unconstrained from the current polarization data. Therefore, we simulate the future Planck and CMBPol data to constrain ϵ further. We find that the future Planck data is very difficult to constrain ϵ , if the primordial tensor perturbations are small, $r < 0.1$. Using the future CMBPol data, the constraint of ϵ can be improved to $\sigma(\epsilon) \sim 0.1$, if the fiducial value $r = 0.3$. We could use the future CMBPol data to verify the gCS model.

Acknowledgements

We acknowledge the use of the Legacy Archive for Microwave Background Data Analysis (LAMBDA). Support for LAMBDA is provided by the NASA Office of Space Science.

-
- [1] M. Li, X. L. Wang, B. Feng, X. Zhang, Phys. Rev. **D65**, 103511 (2002).
 - [2] M. Li, X. Zhang, Phys. Lett. **B573**, 20-26 (2003).
 - [3] H. Li, M. Li, X. Zhang, Phys. Rev. **D70**, 047302 (2004).
 - [4] B. Feng, H. Li, M. Li, X. Zhang, Phys. Lett. **B620**, 27-32 (2005).
 - [5] M. Li, J. Q. Xia, H. Li, X. Zhang, Phys. Lett. **B651**, 357-362 (2007).
 - [6] B. Feng, M. Li, J. Q. Xia, X. Chen, X. Zhang, Phys. Rev. Lett. **96**, 221302 (2006).
 - [7] S. M. Carroll, G. B. Field, R. Jackiw, Phys. Rev. **D41**, 1231 (1990).
 - [8] A. Lue, L. M. Wang, M. Kamionkowski, Phys. Rev. Lett. **83**, 1506-1509 (1999).
 - [9] J. Q. Xia, H. Li, X. Wang, X. Zhang, Astron. Astrophys. **483**, 715 (2008).
 - [10] E. Komatsu *et al.*, Astrophys. J. Suppl. **180**, 330 (2009).
 - [11] J. Q. Xia, H. Li, G. B. Zhao, X. Zhang, Astrophys. J. **679**, L61 (2008).
 - [12] E. Y. S. Wu *et al.*, Phys. Rev. Lett. **102**, 161302 (2009).
 - [13] M. L. Brown *et al.*, Astrophys. J. **705**, 978-999 (2009).
 - [14] E. Komatsu *et al.*, Astrophys. J. Suppl. **192**, 18 (2011).
 - [15] J. Q. Xia, H. Li, X. Zhang, Phys. Lett. **B687**, 129-132 (2010).
 - [16] G. C. Liu, S. Lee, K. W. Ng, Phys. Rev. Lett. **97**, 161303 (2006).
 - [17] J. Q. Xia, H. Li, G. B. Zhao, X. Zhang, Int. J. Mod. Phys. **D17**, 2025 (2008).
 - [18] C. Q. Geng, S. H. Ho, J. N. Ng, JCAP **0709**, 010 (2007); P. Cabella, P. Natoli and J. Silk, Phys. Rev. **D76**, 123014 (2007); V. A. Kostelecky, M. Mewes, Phys. Rev. Lett. **99**, 011601 (2007); T. Kahniashvili, R. Durrer, Y. Maravin, Phys. Rev. **D78**, 123009 (2008); F. Finelli, M. Galaverni, Phys. Rev. **D79**, 063002 (2009); A. Gruppuso, P. Natoli, N. Mandolesi, A. De Rosa, F. Finelli, F. Paci, arXiv:1107.5548 [astro-ph.CO].
 - [19] T. E. Montroy *et al.*, Astrophys. J. **647**, 813 (2006); W. C. Jones *et al.*, Astrophys. J. **647**, 823 (2006); F. Piacentini *et al.*, Astrophys. J. **647**, 833 (2006).
 - [20] H. C. Chiang *et al.*, Astrophys. J. **711**, 1123 (2010).
 - [21] S. Saito, K. Ichiki, A. Taruya, JCAP **0709**, 002 (2007).
 - [22] M. Li, Y. F. Cai, X. Wang, X. Zhang, Phys. Lett. **B680**, 118-124 (2009).
 - [23] V. Gluscevic, M. Kamionkowski, Phys. Rev. **D81**, 123529 (2010).
 - [24] L. Page *et al.*, Astrophys. J. **585**, 566 (2003); L. Page *et al.*, Astrophys. J. Suppl. **170**, 335 (2007).
 - [25] L. Pagano *et al.*, Phys. Rev. **D80**, 043522 (2009).
 - [26] J. R. Hinderks *et al.*, Astrophys. J. **692**, 1221 (2009).

- [27] Planck collaboration, *Planck: the scientific programme*, arXiv:astro-ph/0604069.
- [28] Available at <http://universe.gsfc.nasa.gov/program/inflation.html/>.
- [29] A. Lewis, S. Bridle, Phys. Rev. **D66**, 103511 (2002); Available at <http://cosmologist.info/>.
- [30] M. Zaldarriaga and U. Seljak, Phys. Rev. **D58**, 023003 (1998).